Aerospace Science and Technology 77 (2018) 409–418

Contents lists available at ScienceDirect

Aerospace Science and Technology

www.elsevier.com/locate/aescte

Two-degree-of-freedom attitude tracking control for bank-to-turn aerial vehicles: An additive-state-decomposition-based method

Jinrui Ren [a,*], Quan Quan [a], Li-Bing Zhao [b], Xunhua Dai [a], Kai-Yuan Cai [a]

[a] School of Automation Science and Electrical Engineering, Beihang University, Beijing, 100191, China
[b] China Academy of Aerospace Standardization and Product Assurance, Beijing, 100071, China

ARTICLE INFO

Article history:
Received 26 July 2017
Received in revised form 29 January 2018
Accepted 18 March 2018
Available online 21 March 2018

Keywords:
Bank-to-turn aerial vehicles
Two-degree-of-freedom
Additive state decomposition
Backstepping control
Disturbance rejection

ABSTRACT

This paper presents an additive-state-decomposition-based attitude tracking control method for a class of bank-to-turn aerial vehicles subject to unknown disturbances and nonlinear coupling. This method 'additively' decomposes the original tracking problem into two more tractable problems, namely a tracking problem for a deterministic nonlinear 'primary' system, and a disturbance rejection problem for a linear time-invariant 'secondary' system. Based on the decomposition, a backstepping controller is designed for the primary system to track the reference attitude signal, and a proportional-integral controller is applied to the secondary system to compensate for the disturbances. Finally, the two designed controllers are combined to achieve the original control objective. By using additive state decomposition, the proposed control method with two degrees of freedom can consider tracking task and disturbance rejection task respectively. Simulation results illustrate that the proposed controller can track the reference attitude signal and compensate for disturbances meanwhile. Additionally, the ASD-based controller outperforms the traditional backstepping controller in the presence of unknown disturbances and input delay, and the robustness of the full system can be improved by adjusting the controller parameters of the secondary system.

1. Introduction

It is well-known that the bank-to-turn (BTT) control provides potential performance improvement for aerial vehicles including missiles [1] and unmanned aerial vehicles (UAVs) [2]. Compared with the skid-to-turn (STT) control mode, the BTT control mode provides higher maneuverability, larger acceleration, and faster response. Hence, the autopilot design of BTT aerial vehicles (BTT aerial vehicles denote the aerial vehicles adopting the BTT control mode) has received widespread attention. To perform the control strategies of BTT autopilots, aerial vehicles must have the capability of changing the orientation of acceleration rapidly via a considerably large roll rate. However, such a large roll rate further induces unignorable cross-coupling, which results in undesirable pitch and yaw motions. Furthermore, the imprecise knowledge of aerodynamic parameters, highly nonlinear dynamics, and unknown disturbances make the autopilot design of BTT aerial vehicles more challenging [3,4]. Thus, the autopilot design of BTT aerial vehicles is meaningful.

Various control methods have been applied to the autopilot design of BTT aerial vehicles. The most frequently-used methods can be divided into five categories.

(i) The gain-scheduling control method is adopted by [5–7]. It is a linear control method, which is based on some classical linear control methods, such as linear quadratic regulator, H_∞, μ-synthesis. Two significant limitations of gain-scheduling are that a linearization assumption is needed and parameter variations may be too fast. In order to solve the first limitation, a linear parameter varying (LPV) model is adopted by [7]. However, the control design is separated onto decoupled channels to facilitate the transformation into an LPV form. Since BTT aerial vehicles have high coupling characteristic, the methods aiming at linear independent channel design cannot respond very well due to a large roll rate.

(ii) The input/output feedback linearization control method is one of common nonlinear methods [8,9], which is proposed for multiple-input–multiple-output systems directly. A kind of feedback linearization technique along with a singular perturbation-like technique is adopted by [9], and excellent set-point tracking performance is obtained. The drawbacks of feedback linearization are that an accurate model is often required and the intrinsic singularity problem may occur.

* Corresponding author.
E-mail address: renjinrui@buaa.edu.cn (J. Ren).

https://doi.org/10.1016/j.ast.2018.03.025

(iii) The backstepping control method [2,10] is another choice, which is a systematic approach guaranteeing stability based on Lyapunov functions. However, system performance may deteriorate when model uncertainty is large. In order to solve the problem, robust sigmoid-like control functions are used to confine the uncertain terms [10]. However, in practice, uncertain terms are mostly related to aerodynamic coefficients and dynamic pressure. Therefore, the corresponding bounding functions, which are often constructed using experience or based on a priori knowledge on system behaviors, are difficult to obtain.

(iv) In order to cope with various disturbances, the robust control method including H_∞ [11], μ-synthesis [5], and sliding mode control [12,13] attract researchers' attention. Robust control allows the formulation of the robustness and performance requirements with respect to plant uncertainty or disturbances. The resulting controllers can cover a wider flight envelope and offer a systematic treatment of coupled system dynamics. Nevertheless, robust control is less intuitive than classical control techniques. In addition, a disturbance observer is another choice to improve system robustness [14].

(v) The intelligent control method is also popular, such as fuzzy logic [4,15] or neural networks [3,16] based control methods. Intelligent control can tackle unknown nonlinearities, but the corresponding design is somewhat complicated. The number of fuzzy rules may become prohibitively large and sparse, and neural networks may cost a long time to learn for complex high-dimensional systems.

It is well-known that there is an intrinsic conflict between performance (trajectory tracking) and robustness (disturbance rejection) in the standard feedback framework [17]. This conflict inspires an idea that it would be better to tackle the two control objectives separately. In order to exploit this idea, an additive-state-decomposition-based (ASD-based) [18] attitude tracking control method is proposed for the extended medium range air-to-air technology (EMRAAT) BTT missile, a typical representative of BTT aerial vehicles. The basic idea of the control design is to additively decompose the original tracking problem into two more tractable problems, namely a tracking problem for a deterministic nonlinear primary system and a disturbance rejection problem for a linear time-invariant (LTI) secondary system. Based on the decomposition, a backstepping controller is designed for the tracking problem, and a classical proportional-integral (PI) controller is adopted to solve the disturbance rejection problem for the secondary system. The advantage of the ASD-based control method lies in the decomposition of the original problem into two well-solved control problems. Unlike the aforementioned control methods, the proposed control method avoids model linearization and neglect of nonlinear dynamics as much as possible.

The main contributions of this paper are summarized as below.

(i) An ASD-based control method is proposed to solve the attitude tracking problem for BTT aerial vehicles. Introducing additive state decomposition simplifies the design and also increases the flexibility of controller design.

(ii) The proposed control method is a type of two-degree-of-freedom control method, which separates a disturbance rejection task from a tracking task. Thus, it becomes convenient to consider tracking performance and robustness, respectively, and it is easier to obtain a better comprehensive performance.

(iii) A major difference of this control method from the previous ASD-based control method [18,19] is the tracking task is allocated to a nonlinear system, rather than an LTI system. On the other hand, allocating disturbances to an LTI system makes disturbance rejection more achievable. Moreover, only state feedback controllers are designed for nonlinear subsystems in [18,19], whereas a backstepping controller is adopted for the nonlinear subsystem in this paper.

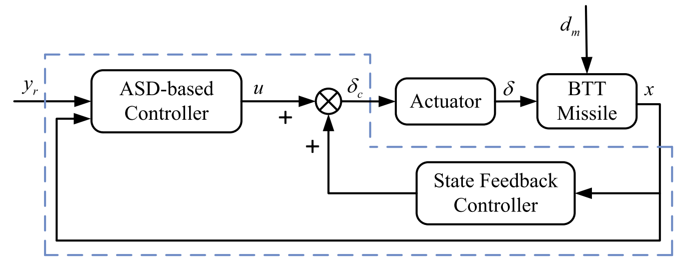

Fig. 1. Schematic diagram of the BTT missile system.

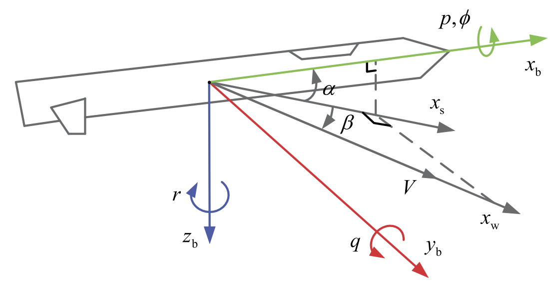

Fig. 2. BTT missile diagram.

The remainder of this paper is organized as follows. In Section 2, an EMRAAT BTT missile model is given. Section 3 presents the ASD-based tracking controller design for the BTT missile. In Section 4, simulations are carried out to demonstrate the effectiveness and robustness of the proposed control method. Section 5 concludes this paper and gives future work.

2. EMRAAT BTT missile model

A schematic diagram of the complete BTT missile system is shown in Fig. 1, where d_m is the disturbance acting on the BTT missile. The BTT missile model will be described in this section, and the BTT autopilot including the state feedback controller and the ASD-based controller will be designed in the subsequent section.

The studied BTT aerial vehicle is an EMRAAT BTT missile, a typical benchmark. When establishing the BTT missile model, three commonly used coordinate frames are the missile-body frame ($o_b x_b y_b z_b$), the wind frame ($o_w x_w y_w z_w$), and the stability frame ($o_s x_s y_s z_s$), which are shown in Fig. 2. Several variables necessary for the later model representation are also displayed in Fig. 2, where α is the angle of attack, β is the sideslip angle, ϕ is the roll angle, p is the roll rate, q is the pitch rate, and r is the yaw rate. The concrete definitions of the mentioned coordinate frames and variables can be found in [20].

The dynamic equations of the EMRAAT BTT missile in a flight condition of Mach 2 and 30,000 ft are given as below

$$
\begin{aligned}
\dot{\alpha} &= q - \tan(\beta)\left[p\cos(\alpha) + r\sin(\alpha)\right] + \frac{0.0166}{\cos(\beta)}\cos(\alpha)\cos(\phi) \\
&\quad - \frac{\cos(\alpha)}{\cos(\beta)}\left(0.092\alpha + 3.654\times10^{-5}q + 0.01516\delta_q\right) \\
\dot{\beta} &= p\sin(\alpha) + (-0.0375\beta - 1.8396\times10^{-6}p \\
&\quad + 0.000504\delta_p - 0.00882\delta_r)\cos(\beta) - r\cos(\alpha) \\
&\quad + 0.0166\sin(\phi)\cos(\beta) \\
\dot{\phi} &= p \\
\dot{p} &= 1.7919\times10^{-5}p^2 + 0.0184q^2 - 0.0184r^2 \\
&\quad - 0.0151pq - 0.0023pr
\end{aligned}
$$

$$
\begin{aligned}
& -0.5qr - 0.2223p - 0.0159q + 0.0823r - 6.4354\alpha \\
& +102.2269\beta - 126.9688\delta_p - 3.1941\delta_q + 97.9748\delta_r \\
\dot{q} &= 0.01p^2 + 7.0814\times 10^{-5}q^2 - 0.01r^2 \\
& -5.3719\times 10^{-4}pq + 0.9922pr \\
& +0.002qr - 8.686\times 10^{-4}p - 0.0621q \\
& +3.0643\times 10^{-4}r - 25.2112\alpha \\
& +0.4018\beta - 0.4956\delta_p - 12.5134\delta_q + 0.3847\delta_r \\
\dot{r} &= 0.0039p^2 - 0.00406q^2 + 1.81\times 10^{-4}r^2 \\
& -0.9771pq + 5.0136\times 10^{-4}pr \\
& +0.0149qr + 0.00404p + 1.4304\times 10^{-4}q \\
& -0.0618r - 0.05806\alpha \\
& +9.8096\beta + 1.7892\delta_p + 0.02882\delta_q + 7.7577\delta_r
\end{aligned} \tag{1}
$$

where δ_p, δ_q and δ_r denote the three virtual control surface deflections that influence the roll, pitch and yaw moments, respectively. Readers can refer to [21] for more details about the BTT missile model. Additionally, each input is effected by an actuator modeled as

$$\underbrace{\begin{bmatrix}\delta_p\\ \delta_q\\ \delta_r\end{bmatrix}}_{\delta} = \frac{e^{-\tau_2 s}}{\tau_1 s+1}\underbrace{\begin{bmatrix}\delta_{pc}\\ \delta_{qc}\\ \delta_{rc}\end{bmatrix}}_{\delta_c} \tag{2}$$

where $\tau_1 = 0.0064$ and $\tau_2 > 0$ will be specified in the simulation.

System (1) exhibits strong coupling and nonlinearity. In order to simplify the design process, some assumptions are made as follows so that a simplified model (3) can be obtained to perform the controller design. However, in the simulation, the dynamic equations in (1) will be used.

Assumption 1. $\delta \approx \delta_c$.

Assumption 2. $\sin\alpha \approx \alpha$, $\sin\beta \approx \tan\beta \approx \beta$, $\cos\alpha \approx \cos\beta \approx 1$, $\alpha^2 \approx 0$, $\beta^2 \approx 0$, $\alpha\beta \approx 0$.

Remark 1. Assumption 1 implies that the actuator dynamics are sufficiently fast compared with that of the BTT missile. Since the angle of attack and sideslip angle of the BTT missile are small, Assumption 2 is also reasonable.

By the assumptions above, the EMRAAT BTT missile model is simplified as

$$
\begin{aligned}
\dot{x} &= A_0 x + B\delta + \psi(x) + d \\
y &= Cx, x(0) = x_0
\end{aligned} \tag{3}
$$

where the state vector $x = [\alpha\ \beta\ \phi\ p\ q\ r]^{\mathrm{T}}$, the output vector $y = [\alpha\ \beta\ \phi]^{\mathrm{T}}$, the input vector $\delta = \left[\delta_p\ \delta_q\ \delta_r\right]^{\mathrm{T}}$, and x_0 is the initial state. All the simplified and ignored quantities from the full system (1) to the simplified system (3) based on Assumptions 1–2 are lumped into the unknown disturbance vector $d = [d_1\ d_2\ 0\ d_3\ d_4\ d_5]^{\mathrm{T}}$, whose true value is small. The matrices A_0, B and C are constant, and $\psi(x)$ is a known nonlinear term with respect to the state x. For more information about this model, please refer to Appendix A.

The control objective is to design a tracking controller δ based on the simplified missile model (3), and then apply the designed controller to the full missile model (1) such that $y - y_r \to 0$ as $t \to \infty$ when there exist disturbances, where y_r is the reference attitude signal.

Remark 2. The formulated control problem is applicable to the attitude tracking control for not only BTT missiles but also BTT UAVs [2] whose dynamic models are in the form of (3).

3. ASD-based tracking controller design

This section presents the BTT autopilot design. First, based on additive state decomposition, the considered system (5) is decomposed into two subsystems: a deterministic nonlinear primary system (9) and an LTI secondary system (10) including all disturbances. Correspondingly, the original tracking task for system (5) is decomposed into two subtasks: a tracking subtask for (9) and a disturbance rejection subtask for (10).

3.1. Additive state decomposition

Additive state decomposition (ASD) [18] is a decomposition method for nonlinear systems just like superposition principle for linear systems. ASD was first proposed in [22], and the latest research can be found in [19]. In the following, ASD is introduced to decompose the aforementioned BTT missile model into two subsystems to make the following controller design more flexible and easier.

In order to obtain a stable system matrix, a simple state feedback controller is designed as

$$\delta = u + Kx \tag{4}$$

where $K \in \mathbb{R}^{3\times 6}$. Since the pair (A_0, B) is controllable, there always exists a matrix K such that $A_0 + BK$ is stable, and the eigenvalues can be assigned freely. After state feedback (4), the simplified BTT model (3) is rewritten as

$$
\begin{aligned}
&\dot{x} = \underbrace{(A_0 + BK)}_{A}x + Bu + \psi(x) + d \\
&y = Cx, x(0) = x_0.
\end{aligned} \tag{5}
$$

Consider system (5) as the original system. By applying ASD, the primary system is chosen as

$$
\begin{aligned}
&\dot{x}_p = Ax_p + Bu_p + \psi(x) \\
&y_p = Cx_p, x_p(0) = x_0
\end{aligned} \tag{6}
$$

where $x_p = \left[\alpha_p\ \beta_p\ \phi_p\ p_p\ q_p\ r_p\right]^{\mathrm{T}}$ and $y_p = \left[\alpha_p\ \beta_p\ \phi_p\right]^{\mathrm{T}}$. Then, subtracting the primary system (6) from the original system (5) gives

$$
\begin{aligned}
&\dot{x} - \dot{x}_p = A\left(x - x_p\right) + B\left(u - u_p\right) + d \\
&y - y_p = C\left(x - x_p\right), x(0) - x_p(0) = 0.
\end{aligned} \tag{7}
$$

Next, by defining

$$x_s = x - x_p,\ y_s = y - y_p,\ u_s = u - u_p \tag{8}$$

system (6) and system (7) become

$$\text{Primary system:} \begin{cases}\dot{x}_p = Ax_p + Bu_p + \psi\left(x_p + x_s\right)\\ y_p = Cx_p, x_p(0) = x_0\end{cases} \tag{9}$$

$$\text{Secondary system:} \begin{cases}\dot{x}_s = Ax_s + Bu_s + d\\ y_s = Cx_s, x_s(0) = 0\end{cases}. \tag{10}$$

The two decomposed systems have the same dimensions with the original system (5). Conversely, the original system (5) can be replaced by putting the primary system (9) and the secondary system (10) together, which means the state and the output satisfy

$$x = x_p + x_s,\ y = y_p + y_s,\ u = u_p + u_s. \tag{11}$$

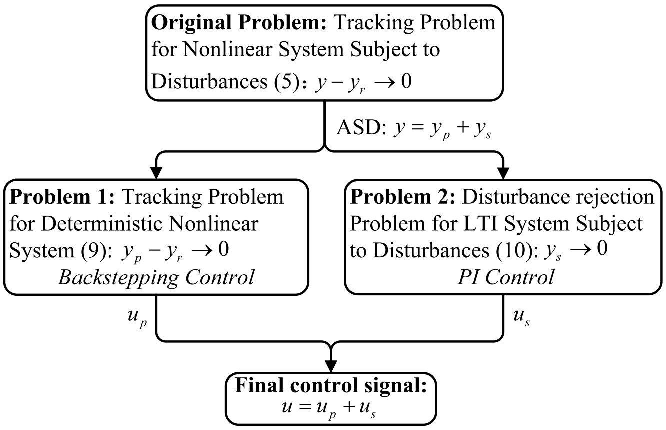

Fig. 3. Additive state decomposition of system (5).

It is clear from equations (9)–(11) that if the controller u_p drives $y_p - y_r \to 0$ as $t \to \infty$ and the controller u_s drives $y_s \to 0$ as $t \to \infty$, then $y - y_r \to 0$ as $t \to \infty$. The strategy here is to assign the tracking subtask to the primary system (9) and the disturbance rejection subtask to the secondary system (10), which is shown in Fig. 3. Since system (9) is a deterministic nonlinear system, many nonlinear tracking control methods, such as the backstepping control method, can be applied to solve the tracking problem. On the other hand, system (10) is a classical LTI system, standard design methods in either frequency domain or time domain, such as the proportional-integral control method, can be used to handle the disturbance rejection problem. It should be noticed that the ASD offers a two-degree-of-freedom way to tackle a tracking task and a disturbance rejection task respectively.

Remark 3. The considered system and the concrete decomposition distinguish from those in [18]. First, the nonlinear function vector $\psi(\cdot)$ in [18] is with respect to the output, whereas $\psi(\cdot)$ is a nonlinear function vector with respect to the state here. Furthermore, the original tracking problem in [18] is decomposed into an output feedback tracking problem for an LTI primary system and a state feedback stabilization problem for a nonlinear secondary system. By contrast, in this study, the considered tracking problem for system (5) is decomposed into a tracking problem for the deterministic nonlinear primary system (9) and a disturbance rejection problem for the LTI secondary system (10).

Remark 4. It can be seen that the disturbances are allocated to the LTI system (10), to which classical robust control methods are applicable. For an LTI system, the development of robust control is rather mature, so the disturbance rejection problem of system (10) is easier than that of the nonlinear system (5).

3.2. Controller design for the primary and secondary systems

So far, the considered system has been decomposed into two subsystems in charge of corresponding subtasks. In this section, controller design is investigated in the form of two problems with respect to the two subtasks, respectively.

3.2.1. Problem 1: tracking problem

For (9), design a controller

$$u_p = u_p\left(x_p, y_r\right) \tag{12}$$

such that $e_p = y_p - y_r \to 0$ as $t \to \infty$, meanwhile keeping x_p bounded.

It is shown from equations (9) and (10) that the secondary system is an independent system which has no relationship with the primary system, whereas the primary system is affected by the secondary system via the term $\psi\left(x_p + x_s\right)$. In order to make the controller design easier, the primary system (9) is further rewritten as

$$\dot{x}_p = Ax_p + Bu_p + \psi\left(x_p\right) + \left[\psi\left(x_p + x_s\right) - \psi\left(x_p\right)\right]. \tag{13}$$

From Appendix A, it can be known that

$$\psi(x) = \left[-p\beta \quad p\alpha \quad 0 \quad 0 \quad 0.01p^2 + 0.9922pr \quad 0.0039p^2 - 0.9771pq\right]^{\mathrm{T}}.$$

Since controller design for the secondary system aims to drive $y_s \to 0$ as $t \to \infty$, namely α_s, β_s and ϕ_s approach to zero. Further, due to the relationship between angles and angular rates, the states p_s, q_s and r_s will tend to small quantities. According to these, $\psi\left(x_p + x_s\right) - \psi\left(x_p\right) \approx 0$ in (13) can be considered during the controller design, because each element in $\psi(x)$ is coupled with attitude angular rates. Thus, *Problem 1* can be solved based on

$$\dot{x}_p = Ax_p + Bu_p + \psi\left(x_p\right). \tag{14}$$

Then, it can be found that equation (14) can be rewritten in a "strict-feedback" form as

$$\dot{x}_{1,p} = \varphi_1\left(x_{1,p}\right) + f_1\left(x_{1,p}\right)x_{2,p} \tag{15}$$

$$\dot{x}_{2,p} = \varphi_2\left(x_{1,p}, x_{2,p}\right) + f_2 u_p \tag{16}$$

$$y_p = x_{1,p} \tag{17}$$

where $x_{1,p} = \left[\alpha_p \ \beta_p \ \phi_p\right]^{\mathrm{T}}$, $x_{2,p} = \left[p_p \ q_p \ r_p\right]^{\mathrm{T}}$, $\varphi_1\left(x_{1,p}\right) \in \mathbb{R}^3$ and $f_1\left(x_{1,p}\right) \in \mathbb{R}^{3\times3}$ are nonlinear function matrices about state $x_{1,p}$, $\varphi_2\left(x_{1,p}, x_{2,p}\right) \in \mathbb{R}^3$ is a nonlinear function matrix about states $x_{1,p}$ and $x_{2,p}$, $f_2 \in \mathbb{R}^{3\times3}$ is a constant matrix, and $x_{2,p}$ is treated as a virtual control input to (15). A well-known control method applicable to "strict-feedback" systems is the backstepping control method, which is a systematic approach guaranteeing stability based on Lyapunov functions. The backstepping control method can achieve good tracking performance with short settling time for nonlinear systems. Moreover, the primary system (9) is a pure system without uncertainties, so the poor robustness problem mentioned in Section 2 will not occur. Thus, the backstepping control method is a good choice to design a controller for (14). It should be noticed that system (14) is just a control-oriented model, and the feedback signals for the backstepping controller still come from system (9) (see Theorem 3 in the following).

Theorem 1. *For system (9), if the backstepping controller is designed as*

$$u_p\left(x_p, y_r\right) = -f_2^{-1}\Bigg(k_2 e_2 + \varphi_2\left(x_{1,p}, x_{2,p}\right) - \frac{\partial x_{2,p,r}}{\partial x_{1,p}^T}\left(\varphi_1\left(x_{1,p}\right) + f_1\left(x_{1,p}\right)x_{2,p}\right) + f_1^T e_1\Bigg) \tag{18}$$

then $y_p - y_r \to 0$ as $t \to \infty$, and x_p is bounded.

Proof.

The basic idea of the proof follows [23], and the concrete proof can be found in Appendix B. The backstepping controller design process is also provided. □

3.2.2. Problem 2: disturbance rejection problem

For (10), design a disturbance rejection controller

$$u_s = u_s\left(x_s, \int_0^t y_s(s)\,\mathrm{d}s\right) \tag{19}$$

such that $y_s \to 0$ as $t \to \infty$, meanwhile keeping x_s bounded.

In the following, a proportional-integral controller will be designed. Define a new variable $z(t) = \int_0^t y_s(s)\mathrm{d}s$. Then

$$\dot{z} = Cx_s. \tag{20}$$

By using (20), system (10) can be augmented as

$$\begin{bmatrix} \dot{z} \\ \dot{x}_s \end{bmatrix} = \begin{bmatrix} 0 & C \\ 0 & A \end{bmatrix}\begin{bmatrix} z \\ x_s \end{bmatrix} + \begin{bmatrix} 0 \\ B \end{bmatrix} u_s + \begin{bmatrix} 0 \\ d \end{bmatrix} \tag{21}$$

$$y_s = \begin{bmatrix} 0 & C \end{bmatrix}\begin{bmatrix} z \\ x_s \end{bmatrix}. \tag{22}$$

Theorem 2. *For the augmented system (21), if i) d is a constant vector, ii) there exists a control input*

$$u_s = \bar{K}_1 z + \bar{K}_2 x_s \tag{23}$$

where $\bar{K}_1 \in \mathbb{R}^{3\times 3}$ and $\bar{K}_2 \in \mathbb{R}^{3\times 6}$, such that

$$A_a = \begin{bmatrix} 0 & C \\ 0 & A \end{bmatrix} + \begin{bmatrix} 0 \\ B \end{bmatrix}\begin{bmatrix} \bar{K}_1 & \bar{K}_2 \end{bmatrix} \tag{24}$$

is stable, then $y_s(t) \to 0$ as $t \to \infty$, and x_s is bounded.

Proof. The basic idea of the proof follows [24], and the concrete proof can be found in Appendix C. □

In this paper, the disturbance vector d in (10) is considered as a slow time-varying signal. Therefore, the disturbance rejection controller for the secondary system (10) is designed as

$$u_s\left(x_s, \int_0^t y_s(s)\,\mathrm{d}s\right) = \bar{K}_1 \int_0^t y_s(s)\,\mathrm{d}s + \bar{K}_2 x_s. \tag{25}$$

3.3. Controller integration

Controller design for the decomposed systems (9) and (10) requires their states and outputs as feedback variables. However, they are virtual and unknown. For such a purpose, an observer is designed in Theorem 3 to estimate x_p, x_s and y_s.

Theorem 3. *Suppose that an observer is designed to estimate x_p, x_s and y_s in (9) and (10) as*

$$\dot{\hat{x}}_p = A\hat{x}_p + Bu_p + \psi(x), \hat{x}_p(0) = x_0. \tag{26}$$

$$\hat{x}_s = x - \hat{x}_p \tag{27}$$

$$\hat{y}_s = C\hat{x}_s. \tag{28}$$

Then $\hat{x}_p \equiv x_p$, $\hat{x}_s \equiv x_s$ and $\hat{y}_s \equiv y_s$.

Proof. Subtracting (26) from (9) results in $\dot{\tilde{x}}_p = A\tilde{x}_p$ and $\tilde{x}_p(0) = 0$, where $\tilde{x}_p \triangleq x_p - \hat{x}_p$. Then, considering that A is stable, $\tilde{x}_p \equiv 0$, which implies that $\hat{x}_p \equiv x_p$. Consequently, by (11), it can be obtained that $\hat{x}_s \equiv x - \hat{x}_p \equiv x_s$. Additionally, $\hat{y}_s \equiv C\hat{x}_s \equiv y_s$. □

Remark 5. The designed observer is an open-loop observer, in which A must be stable. Otherwise, state feedback is needed to obtain a stable A, which can be realized by controller (4). If a closed-loop observer is adopted here, then it will be rather difficult to analyze the stability of the closed-loop system consisting of the nonlinear controller and observer, because separation principle does not hold in nonlinear systems.

Remark 6. Since the initial values $x_p(0)$ and $\hat{x}_p(0)$ are both assigned by the designer, they are all deterministic. If there is an initial value measurement error, then it will be assigned to and considered in the secondary system in the form of disturbances.

With the solutions to the two problems in hand, one is ready to claim Theorem 4.

Theorem 4. *Under Assumptions 1 and 2, suppose (i) Problems 1 and 2 are solved; (ii) the controller for system (1) is designed as*

Observer:

$$\begin{aligned} &\dot{\hat{x}}_p = A\hat{x}_p + Bu_p + \psi(x), \hat{x}_p(0) = x_0 \\ &\hat{x}_s = x - \hat{x}_p \\ &\hat{y}_s = C\hat{x}_s \end{aligned} \tag{29}$$

Controller:

$$\delta_c = u_p(\hat{x}_p, y_r) + u_s\left(\hat{x}_s, \int_0^t \hat{y}_s(s)\,ds\right) + Kx. \tag{30}$$

Then, the output of system (1) satisfies $y - y_r \to 0$ as $t \to \infty$.

Proof. According to Theorem 3, observer (29) will make $\hat{x}_p \equiv x_p$, $\hat{x}_s \equiv x_s$ and $\hat{y}_s \equiv y_s$. Under condition (i), the controller u_p drives $y_p - y_r \to 0$ as $t \to \infty$ for system (9) (Theorem 1), and the controller u_s drives $y_s(t) \to 0$ as $t \to \infty$ for system (10) (Theorem 2). Then the controller $u = u_p + u_s$ guarantees $y - y_r \to 0$ as $t \to \infty$ for system (5). Moreover, taking the state feedback into consideration, the controller (30) guarantees $y - y_r \to 0$ as $t \to \infty$ for system (1). □

The structure of the overall closed-loop system is depicted in Fig. 4.

Remark 7. In Fig. 4, the dash-dotted line represents the unidirectional interaction between the primary system and the secondary system. If $x_s = 0$, then the two systems are completely decoupled, and the primary system is a pure system. Otherwise, the secondary system affects the primary system by the coupling term $\psi(x_p + x_s)$. As long as the controller of the secondary system is well designed, $x_s \to 0$ in a short time, namely $\psi(x_p + x_s) \to \psi(x_p)$ fast. Thus, it can be roughly considered that the two systems are decoupled. In this case, a resulting thought comes that one can improve the tracking performance of the primary system and the disturbance rejection performance of the secondary system, respectively. In the following, the disturbance rejection performance improvement of the full system by just adjusting the controller parameters of the secondary system is studied in the simulation.

4. Simulation studies

In this section, the effectiveness, robustness, and practicality of the proposed method are demonstrated through various simulations and analyses. The closed-loop responses to the desired

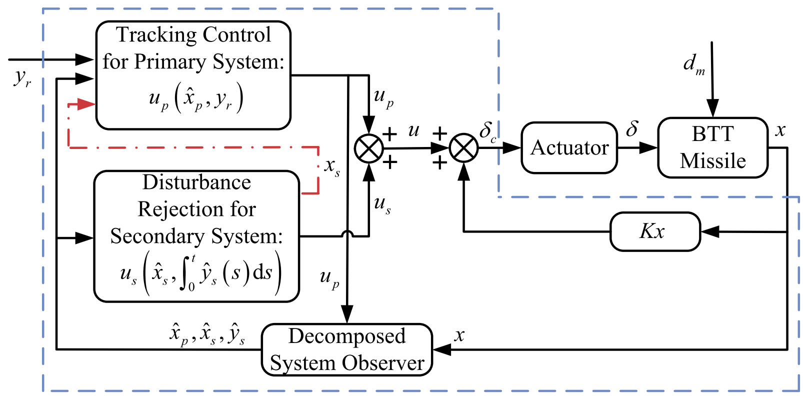

Fig. 4. Structure of the closed-loop system with the ASD-based control.

attitude command are simulated with the full nonlinear plant (1) considering the actuators' dynamics and saturation. Moreover, the robustness against disturbances and delay is investigated, and the problem about how to obtain stronger robustness is also studied.

4.1. Parameter settings

In the simulation, some controller parameters are selected as follows. The reference attitude $y_r = [5° \ 0° \ 45°]^{\mathrm{T}}$. The initial states $\alpha_0 = 1°$, $\beta_0 = 0.11°$, $\phi_0 = 5°$, $p_0 = 0°/\mathrm{s}$, $q_0 = 0°/\mathrm{s}$, $r_0 = 0°/\mathrm{s}$. Choose

$$K = \begin{bmatrix} 0.013 & -0.073 & -0.017 & -0.011 & 0.008 & -0.160 \\ -1.938 & 0.007 & -0.022 & -0.017 & 0.170 & -0.008 \\ 0.023 & -1.134 & -0.033 & -0.036 & 0.018 & -0.212 \end{bmatrix}$$

then $A = A_0 + BK$ is stable, whose eigenvalues are $-0.5, -0.7, -0.9, -1.2, -1.5, -1.8$. For the backsteping controller (18), $k_1 = 30$ and $k_2 = 35$. For the PI controller (25), the feedback gain matrices are designed as

$$\bar{K}_1 = \begin{bmatrix} -0.841 & 38.769 & 1.997 \\ 39.771 & -0.413 & -1.935 \\ 0.437 & 50.414 & -2.163 \end{bmatrix},$$

$$\bar{K}_2 = \begin{bmatrix} -0.338 & 14.955 & 0.930 & 0.147 & -0.051 & -1.789 \\ 14.834 & -0.111 & -0.491 & -0.020 & 1.722 & 0.015 \\ 0.101 & 19.421 & -0.626 & -0.024 & -0.009 & -2.317 \end{bmatrix}.$$

Then, the eigenvalues of A_a are $-7, -7.2, -7.4, -7.6, -7.8, -8, -8.2, -8.4, -8.6$. Additionally, the saturation constraint of the control input δ_c is selected as $[-40°, 40°]$.

4.2. Compared method

In order to verify the tracking performance and robustness of the ASD-based tracking control method, comparisons are also made between the ASD-based tracking control method and a traditional backstepping control method. A traditional backstepping controller is designed as

$$\bar{\delta}_c = u_p(x, y_r) + Kx. \tag{31}$$

The structure of the closed-loop system with backstepping controller (31) is presented in Fig. 5. It should be noticed that, in the proposed controller (30), $\hat{x}_p$ replaces x in $u_p(x, y_r)$.

4.3. Results

4.3.1. Simulation of performance

In the first group of simulations, the nominal case, which does not consider disturbances and delay, is studied. In the nominal case, the control performance is not affected by the disturbance rejection performance, and thus can be better shown. The designed two controllers are directly applied to the full model (1). The system outputs are presented in Fig. 6, and the corresponding control inputs are presented in Fig. 7. It is obvious that both methods can achieve the control objective given in Section 2. Although the ASD-based controller leads to a little slower tracking response than the traditional backstepping controller, the control inputs of the traditional backstepping controller are larger and even reach the saturation bound.

In order to reveal the actual role of the primary and secondary systems, the corresponding responses are shown in Fig. 8. The responses are consistent with the theoretical analyses that the primary system performs a tracking task, and the secondary system performs a stabilization task.

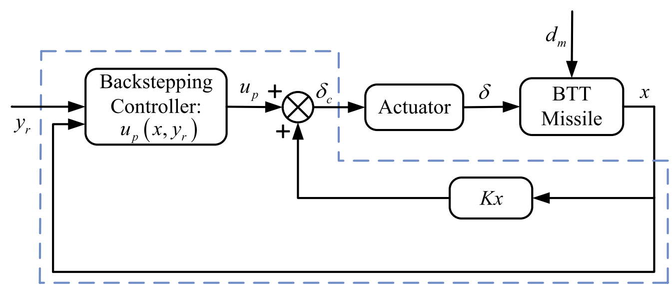

Fig. 5. Structure of the closed-loop system with the traditional backstepping control.

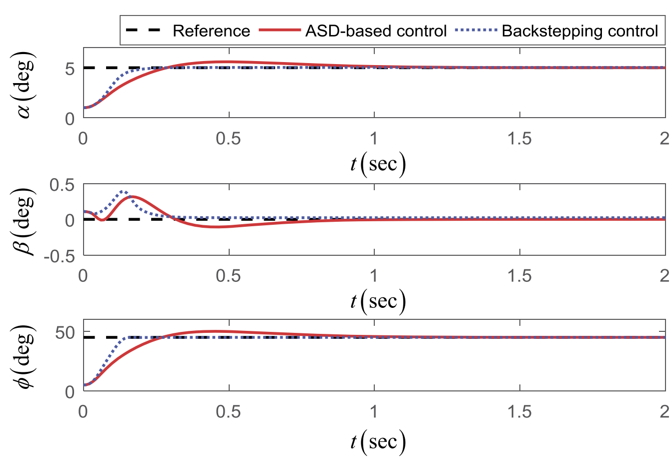

Fig. 6. System outputs.

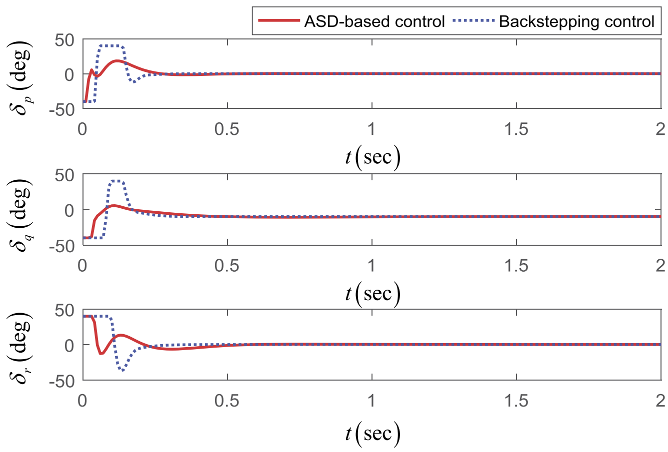

Fig. 7. Control inputs.

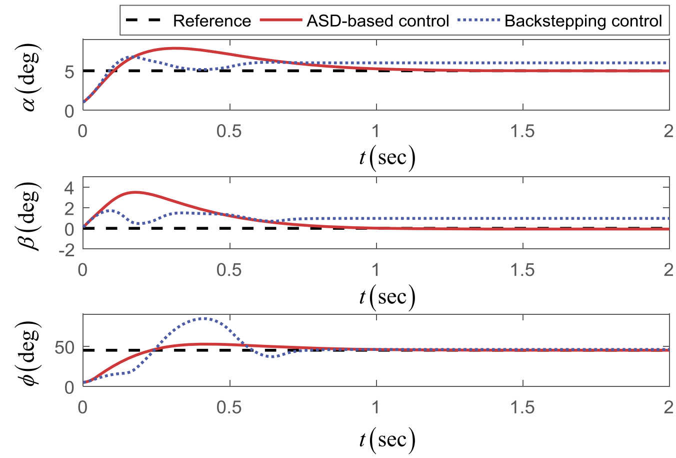

Fig. 9. System response subject to disturbance $d1$.

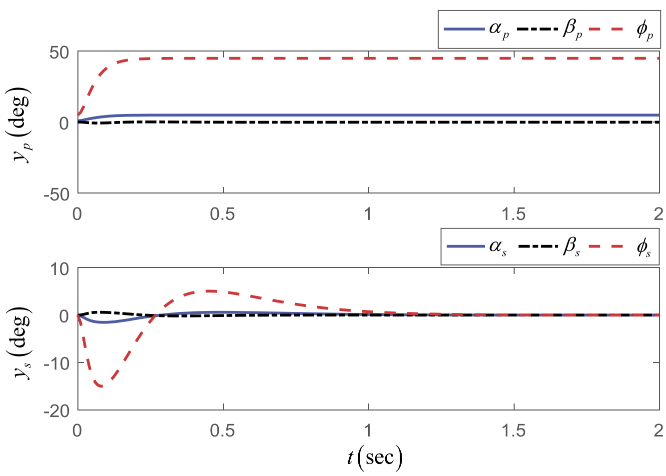

Fig. 8. System responses of the primary and secondary systems.

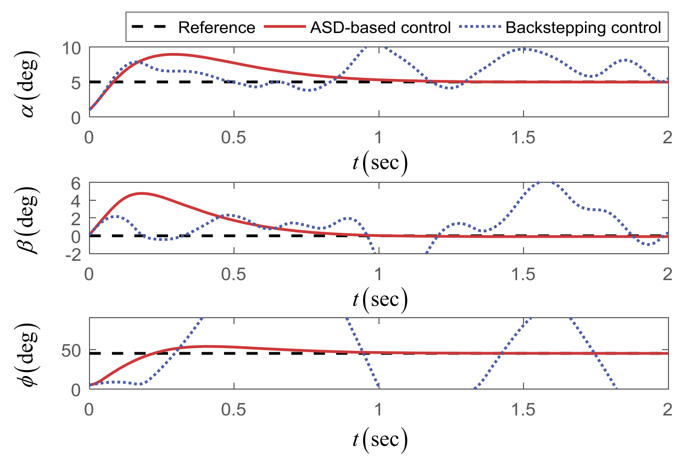

Fig. 10. System response subject to disturbance $d2$.

4.3.2. Simulation of robustness

In the second group of simulations, some other cases, which take disturbances or delay into consideration, are studied with the full model (1). In these cases, the disturbance rejection performance of the proposed controller can be displayed by comparing with the nominal case and the traditional backstepping controller.

In order to test the inherent robustness of the designed controllers, system (1) is perturbed by disturbance first $d1 = [0.5\ 0.5\ 0.5\ 0.5\ 0.5\ 0.5]^{\mathrm{T}}$, and then $d2 = [0.7\ 0.7\ 0.7\ 0.7\ 0.7\ 0.7]^{\mathrm{T}}$. The disturbance $d1$ or $d2$ is a lumped one including system disturbance, measurement noise, and model uncertainty, which corresponds to d_m in Fig. 1 and Fig. 4. It is evident from Fig. 9 that, when there exists disturbance $d1$, the response of the ASD-based controller is still smooth, while the traditional backstepping controller leads to system oscillation and the outputs cannot finally converge to the desired values. When the disturbance is further increased to $d2$, Fig. 10 shows that the traditional backstepping controller causes system divergence, whereas the ASD-based controller still performs well.

Remark 8. The traditional backstepping control method results in system oscillation, system divergence and nonzero steady-state error when there exist disturbances. The reason is that equation (B.11) becomes $\dot{V}_2 = -k_1 e_1^{\mathrm{T}} e_1 - k_2 e_2^{\mathrm{T}} e_2 + e_1^{\mathrm{T}} d_1' + e_2^{\mathrm{T}} d_2'$ when there exist disturbances, where d_1' and d_2' are the disturbances existing in the first layer and the second layer of the two-layer strict-feedback system respectively. If the disturbances are small, $\dot{V}_2 < 0$ may still hold, whereas $e_1, e_2 \to 0$ cannot be guaranteed, which is reflected in the system response by a convergence with a nonzero steady-state error. What is worse, if the disturbances are large enough, $\dot{V}_2 > 0$ and the system response is divergent. However, for the ASD-based control method, the primary system is roughly a pure system without disturbances, so the tracking performance can be guaranteed. Furthermore, the PI controller for the secondary system can compensate for the disturbances.

Additionally, the input delay is another common and inevitable phenomenon in practice, so $\tau_2 = 0.015$ sec is considered in Fig. 11. The traditional backstepping controller leads to system oscillation, while the control effect of the ASD-based controller does not change too much compared with the nominal case. As shown in Fig. 12, the traditional backstepping controller destabilizes the closed-loop system as the input delay τ_2 increases to 0.025 s. However, the ASD-based controller still works well.

In order to show the disturbance rejection capability of the secondary system more intuitively, an input disturbance in the form of $d3 = [0\ 0\ 0\ d_W\ d_W\ d_W]^{\mathrm{T}}$ is considered, where d_W is given by a MATLAB/SIMULINK block named Band-Limited White Noise. Two cases are studied here. In Case 1, the noise power of d_W is selected as 0.1. It is shown in Fig. 13 that the response of the primary system is roughly the same as that of the nominal case shown in Fig. 8. Another obvious result is that the oscillation of the full system is nearly the same as that of the secondary system. In Case 2, the noise power of d_W is selected as 1 (Fig. 14). A similar re-

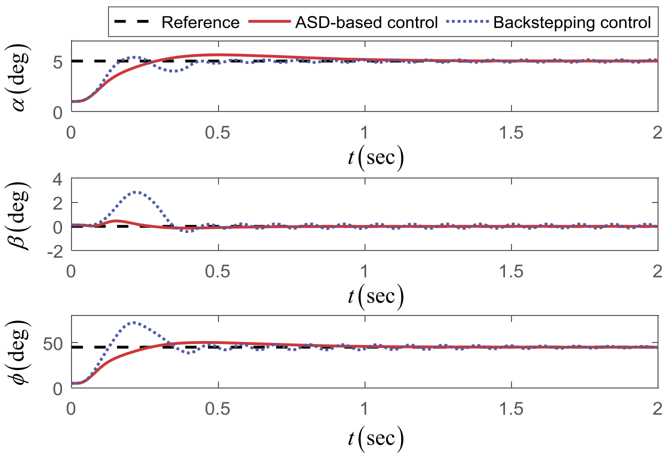

Fig. 11. System response subject to input delay $\tau_2 = 0.015$ s.

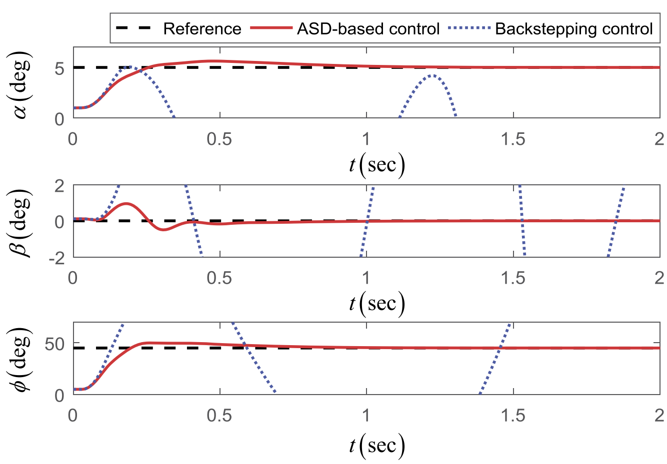

Fig. 12. System response subject to input delay $\tau_2 = 0.025$ s.

sult can be obtained as Case 1, except that the oscillations of the full system and the secondary system become larger than Case 1. Thus, a conclusion can be drawn that the disturbances are allocated to the secondary system leaving the primary system a pure one, which is consistent with the theoretical analyses of Remark 4 and Remark 7. Then, the disturbance rejection performance is improved by adjusting the controller parameters of the secondary system in Case 1 to

$$\bar{K}_1 = \begin{bmatrix} -5.841 & 316.648 & 20.447 \\ 295.621 & -0.474 & 1.168 \\ 1.675 & 410.849 & -11.420 \end{bmatrix},$$

$$\bar{K}_2 = \begin{bmatrix} -1.212 & 60.931 & 4.265 & 0.303 & -0.091 & -3.767 \\ 56.951 & -0.063 & 0.098 & 0.012 & 3.528 & 0.009 \\ 0.233 & 79.022 & -1.809 & -0.059 & -0.006 & -4.880 \end{bmatrix}.$$

This case is denoted as Case 3. It can be found from Fig. 15 that the oscillation of the full system becomes smaller compared with Case 1.

4.4. Discussions

Simulation results present that the ASD-based controller can track the reference attitude signal without steady-state error in the presence of disturbances. Moreover, the ASD-based controller can tolerate larger disturbances and input delay than the traditional backstepping controller. Tracking performance for the primary system is almost maintained in the presence of input disturbances,

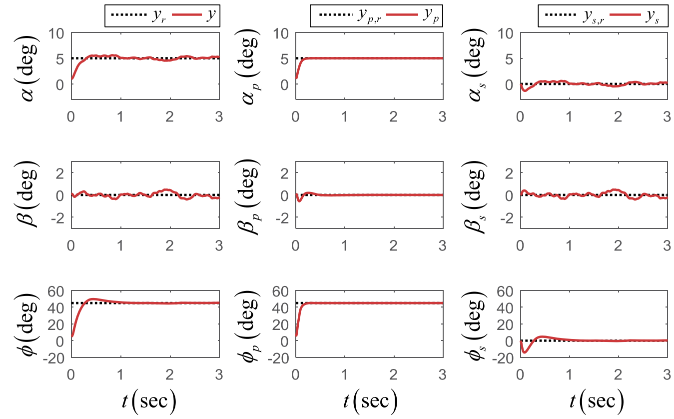

Fig. 13. System responses in Case 1.

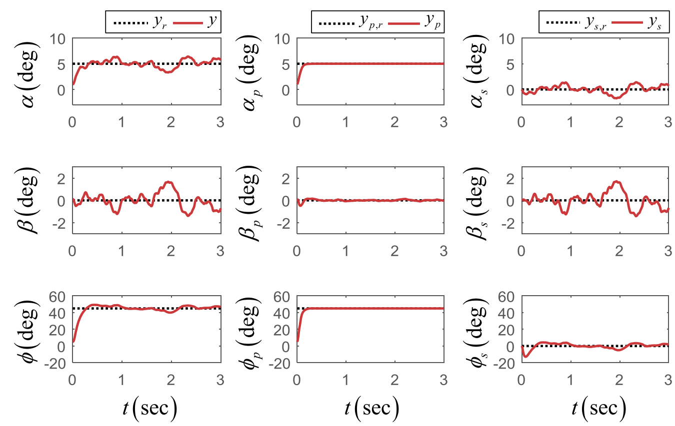

Fig. 14. System responses in Case 2.

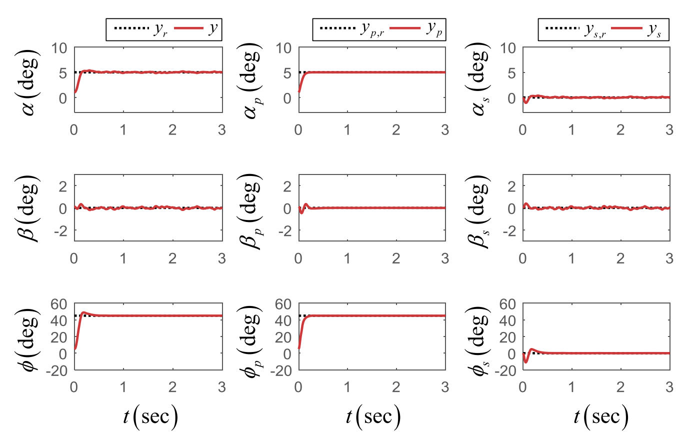

Fig. 15. System responses in Case 3.

and oscillation caused by input disturbances nearly comes from the outputs of the secondary system. It verifies that the primary and secondary systems are roughly decoupled, which leads to an advantage that disturbance rejection effect can be improved by adjusting the controller parameters of the secondary system, leaving the tracking performance unaffected. Since the traditional backstepping control method mixes tracking and disturbance rejection together, the price to be paid is poor robustness against disturbances and delay. By contrast, the ASD-based control method decomposes the tracking task and disturbance rejection task, then one can design a controller for each task respectively. The ASD-based control method with two degrees of freedom can resolve the conflict between the reference tracking objective and its competing objectives [25]. Therefore, the ASD-based control method can achieve a better tradeoff between tracking performance and robustness.

5. Conclusions

In this study, the attitude tracking problem for a class of BTT aerial vehicles subject to unknown disturbances and nonlinear coupling has been addressed by an ASD-based control method. In order to demonstrate its effectiveness, the control method is applied to the EMRAAT BTT missile. The designed controller can track the reference attitude signal and compensate for unknown disturbances. Simulations show that the ASD-based controller outperforms the traditional backstepping controller in the presence of unknown disturbances and input delay. The robustness of the full system can be improved by adjusting the controller parameters of the secondary system. While PI control and backstepping control are not new, the salient feature of the proposed control method lies in the fusion of them by using additive state decomposition to solve a challenging nonlinear tracking problem. In future research, stability margin could be introduced into the secondary system to study the stability and robustness of the full system in a more accurate and quantitative way. Furthermore, frequency-domain compensation methods could be introduced into the secondary system to study the robustness performance improvement of the full system.

Funding

This work was supported by the National Key Project of Research and Development Plan under Grant 2016YFC1402500 and the National Natural Science Foundation of China under Grant 61473012.

Conflict of interest statement

There is no conflict of interest.

Appendix A. System information about model (3)

$$A_0=\begin{bmatrix} -0.092 & 0 & 0 & 0 & 1 & 0\\ 0 & -0.0375 & 0 & 0 & 0 & -1\\ 0 & 0 & 0 & 1 & 0 & 0\\ -6.4354 & 102.2269 & 0 & -0.2223 & 0 & 0\\ -25.2112 & 0.4018 & 0 & 0 & -0.0621 & 0\\ 0 & 9.8096 & 0 & 0 & 0 & -0.0618 \end{bmatrix},$$

$$B=\begin{bmatrix} 0 & 0 & 0\\ 0 & 0 & 0\\ 0 & 0 & 0\\ -126.9688 & -3.1941 & 97.9748\\ -0.4956 & -12.5134 & 0.3847\\ 1.7892 & 0.02882 & 7.7577 \end{bmatrix},$$

$$\psi(x)=\begin{bmatrix} -p\beta\\ p\alpha\\ 0\\ 0\\ 0.01p^2+0.9922pr\\ 0.0039p^2-0.9771pq \end{bmatrix},$$

$$C=\begin{bmatrix} 1 & 0 & 0 & 0 & 0 & 0\\ 0 & 1 & 0 & 0 & 0 & 0\\ 0 & 0 & 1 & 0 & 0 & 0 \end{bmatrix}.$$

Appendix B. Backstepping controller design for the primary system

The overall design procedure can be divided into three steps.

Step 1. By considering the two-layer feedback system (15)–(17), error variables $e_1, e_2 \in \mathbb{R}^3$ are defined as

$$e_1 = x_{1,p} - x_{1,p,r} \tag{B.1}$$

$$e_2 = x_{2,p} - x_{2,p,r} \tag{B.2}$$

where $x_{1,p,r}$ and $x_{2,p,r}$ are the desired states, $x_{1,p,r}$ is obtained from the reference attitude y_r (here $x_{1,p,r} = y_r$), and $x_{2,p,r}$ will be obtained from the backstepping controller design. The rest steps of the design are to stabilize the two error variables in a recursive manner. Here, by substituting (15)–(16) into (B.1)–(B.2), the error model can be obtained as

$$\dot{e}_1 = \varphi_1\left(x_{1,p}\right) + f_1\left(x_{1,p}\right)x_{2,p} - \dot{x}_{1,p,r} \tag{B.3}$$

$$\dot{e}_2 = \varphi_2\left(x_{1,p}, x_{2,p}\right) + f_2 u_p - \dot{x}_{2,p,r}. \tag{B.4}$$

Step 2. A Lyapunov function is chosen as

$$V_1\left(x_{1,p}\right) = \frac{1}{2}e_1^{\mathrm{T}}e_1. \tag{B.5}$$

Explore a desired virtual control input $x_{2,p,r}$ to make the derivative of (B.5) nonnegative, that is

$$\dot{V}_1\left(x_{1,p}\right) = e_1^{\mathrm{T}}\dot{e}_1 = e_1^{\mathrm{T}}\left(\varphi_1\left(x_{1,p}\right) + f_1\left(x_{1,p}\right)x_{2,p} - \dot{x}_{1,p,r}\right) \le 0. \tag{B.6}$$

In order to make equation (B.6) hold, $x_{2,p,r}$ can be chosen as

$$x_{2,p,r} = -f_1^{-1}\left(x_{1,p}\right)\left(\varphi_1\left(x_{1,p}\right) - \dot{x}_{1,p,r} + k_1 e_1\right) \tag{B.7}$$

where parameter $k_1 > 0$. Then, by putting the desired virtual control input (B.7) into (B.3) and (B.6), one can get

$$\dot{V}_1 = -k_1 e_1^{\mathrm{T}}e_1 + e_1^{\mathrm{T}}f_1 e_2,$$

where the coupling term $e_1^{\mathrm{T}}f_1 e_2$ will be canceled in the next step.

Step 3. Another Lyapunov function is defined as

$$V_2\left(x_{1,p}, x_{2,p}\right) = V_1\left(x_{1,p}\right) + \frac{1}{2}e_2^{\mathrm{T}}e_2. \tag{B.8}$$

The derivative of $V_2\left(x_{1,p}, x_{2,p}\right)$ is

$$\begin{aligned}\dot{V}_2\left(x_{1,p}, x_{2,p}\right) &= \dot{V}_1\left(x_{1,p}\right) + e_2^{\mathrm{T}}\dot{e}_2 = -k_1 e_1^{\mathrm{T}}e_1 + e_1^{\mathrm{T}}f_1 e_2\\ &\quad + e_2^{\mathrm{T}}\left(\varphi_2\left(x_{1,p}, x_{2,p}\right) + f_2 u_p - \dot{x}_{2,p,r}\right).\end{aligned} \tag{B.9}$$

In order to make (B.9) nonnegative, the real control input u_p is selected as

$$\begin{aligned}u_p\left(x_p, y_r\right) = -f_2^{-1}\Bigg(&k_2 e_2 + \varphi_2\left(x_{1,p}, x_{2,p}\right)\\ &- \frac{\partial x_{2,p,r}}{\partial x_{1,p}^{\mathrm{T}}}\left(\varphi_1\left(x_{1,p}\right) + f_1\left(x_{1,p}\right)x_{2,p}\right) + f_1^{\mathrm{T}}e_1\Bigg)\end{aligned} \tag{B.10}$$

where parameter $k_2 > 0$. Then, putting the control input (B.10) into (B.4) and (B.9) results in

$$\dot{V}_2 = -k_1 e_1^{\mathrm{T}}e_1 - k_2 e_2^{\mathrm{T}}e_2 \le 0. \tag{B.11}$$

Hence, $x_{2,p} \to x_{2,p,r}$ and $x_{1,p} \to x_{1,p,r}$ as $t \to \infty$, namely $y_p - y_r \to 0$ as $t \to \infty$, and x_p is bounded.

Remark 9. By the definitions of $f_1(x_{1,p})$ and f_2, one has

$$\det\left(f_1\left(x_{1,p}\right)\right) = \det\left(\begin{bmatrix} -\beta_p & 1 & 0 \\ \alpha_p & 0 & -1 \\ 1 & 0 & 0 \end{bmatrix}\right) = -1$$

and f_2 is a constant matrix with $\det(f_2) \neq 0$. Therefore, the inverse matrices $f_1^{-1}(x_{1,p})$ and f_2^{-1} always exist, and then controller (B.10) is realizable.

Appendix C. Proof of Theorem 2

Substituting the control input (23) into system (21) results in

$$\begin{bmatrix} \dot{z} \\ \dot{x}_s \end{bmatrix} = \begin{bmatrix} 0 & C \\ B\bar{K}_1 & A + B\bar{K}_2 \end{bmatrix} \begin{bmatrix} z \\ x_s \end{bmatrix} + \begin{bmatrix} 0 \\ d \end{bmatrix}. \tag{C.1}$$

By doing Laplace transformation for (C.1), one can get

$$\begin{bmatrix} z(s) \\ x_s(s) \end{bmatrix} = \begin{bmatrix} sI & -C \\ -B\bar{K}_1 & sI - \left(A + B\bar{K}_2\right) \end{bmatrix}^{-1} \begin{bmatrix} 0 \\ d \end{bmatrix} \frac{1}{s}.$$

Since $\begin{bmatrix} 0 & C \\ 0 & A \end{bmatrix} + \begin{bmatrix} 0 \\ B \end{bmatrix} \bar{K}$ is stable, on the basis of the final value theorem, it can be obtained that

$$\begin{aligned} \lim_{t\to\infty} \begin{bmatrix} z(t) \\ x_s(t) \end{bmatrix} &= \lim_{s\to 0} s \begin{bmatrix} z(s) \\ x_s(s) \end{bmatrix} \\ &= \begin{bmatrix} 0 & -C \\ -B\bar{K}_1 & -\left(A + B\bar{K}_2\right) \end{bmatrix}^{-1} \begin{bmatrix} 0 \\ d \end{bmatrix} \end{aligned}$$

which means $x_s(t)$ and $z(t)$ will approach to constants. Thus, $y_s \to 0$ $(\dot{z} = y_s)$ as $t \to \infty$, and x_s is bounded.

References

[1] A.A. Rodriguez, Y. Wang, Performance enhancement methods for unstable bank-to-turn (BTT) missiles with saturating actuators, Int. J. Control 63 (4) (1996) 641–678.
[2] D. Jung, P. Tsiotras, Bank-to-turn control for a small UAV using backstepping and parameter adaptation, IFAC Proc. Vol. 41 (2) (2008) 4406–4411.
[3] L.-C. Fu, W.-D. Chang, J.-H. Yang, T.-S. Kuo, Adaptive robust bank-to-turn missile autopilot design using neural networks, J. Guid. Control Dyn. 20 (2) (1997) 346–354.
[4] C.-K. Lin, Mixed H_2/H_∞ autopilot design of bank-to-turn missiles using fuzzy basis function networks, Fuzzy Sets Syst. 158 (20) (2007) 2268–2287.
[5] S. Theodoulis, F. Sève, P. Wernert, Robust gain-scheduled autopilot design for spin-stabilized projectiles with a course-correction fuze, Aerosp. Sci. Technol. 42 (2015) 477–489.
[6] R.A. Nichols, R.T. Reichert, W.J. Rugh, Gain scheduling for H_∞ controllers: a flight control example, IEEE Trans. Control Syst. Technol. 1 (2) (1993) 69–79.
[7] L.H. Carter, J.S. Shamma, Gain-scheduled bank-to-turn autopilot design using linear parameter varying transformations, J. Guid. Control Dyn. 19 (5) (1996) 1056–1063.
[8] J. Ko, T.W. Strganac, A.J. Kurdila, Adaptive feedback linearization for the control of a typical wing section with structural nonlinearity, Nonlinear Dyn. 18 (3) (1999) 289–301.
[9] S.-Y. Lee, J.-I. Lee, I.-J. Ha, Nonlinear autopilot for high maneuverability of bank-to-turn missiles, IEEE Trans. Aerosp. Electron. Syst. 37 (4) (2001) 1236–1252.
[10] G. Mattei, S. Monaco, Nonlinear autopilot design for an asymmetric missile using robust backstepping control, J. Guid. Control Dyn. 37 (5) (2014) 1462–1476.
[11] S. Kang, H.J. Kim, J.-I. Lee, B.-E. Jun, M.-J. Tahk, Roll-pitch-yaw integrated robust autopilot design for a high angle-of-attack missile, J. Guid. Control Dyn. 32 (5) (2009) 1622.
[12] J. Yao, X. Zhu, Z. Zhou, The design of sliding mode control system based on backstepping theory for BTT UAV, Control Intell. Syst. 36 (4) (2008) 347.
[13] Y. Ma, J. Guo, S. Tang, High angle of attack command generation technique and tracking control for agile missiles, Aerosp. Sci. Technol. 45 (2015) 324–334.
[14] S. Li, J. Yang, Robust autopilot design for bank-to-turn missiles using disturbance observers, IEEE Trans. Aerosp. Electron. Syst. 49 (1) (2013) 558–579.
[15] C.-K. Lin, Adaptive critic autopilot design of bank-to-turn missiles using fuzzy basis function networks, IEEE Trans. Syst. Man Cybern., Part B, Cybern. 35 (2) (2005) 197–207.
[16] C.-K. Lin, S.-D. Wang, An adaptive H-infinity controller design for bank-to-turn missiles using ridge gaussian neural networks, IEEE Trans. Neural Netw. 15 (6) (2004) 1507–1516.
[17] K. Zhou, J.C. Doyle, K. Glover, et al., Robust and Optimal Control, Prentice–Hall, New Jersey, 1996.
[18] Q. Quan, K.-Y. Cai, H. Lin, Additive-state-decomposition-based tracking control framework for a class of nonminimum phase systems with measurable nonlinearities and unknown disturbances, Int. J. Robust Nonlinear Control 25 (2) (2015) 163–178.
[19] Z.-B. Wei, Q. Quan, K.-Y. Cai, Output feedback ILC for a class of nonminimum phase nonlinear systems with input saturation: an additive-state-decomposition-based method, IEEE Trans. Autom. Control 62 (1) (2017) 502–508.
[20] B.L. Stevens, F.L. Lewis, E.N. Johnson, Aircraft Control and Simulation: Dynamics, Controls Design, and Autonomous Systems, John Wiley & Sons, 2015.
[21] D.A. Schumacher, Tactical Missile Autopilot Design Using Nonlinear Control, Ph.D. Thesis, University of Michigan, 1994.
[22] Q. Quan, K.-Y. Cai, Additive decomposition and its applications to internal-model-based tracking, in: Proceedings of the 48th IEEE Conference on Decision and Control, 2009 Held Jointly with the 2009 28th Chinese Control Conference, CDC/CCC 2009, IEEE, 2009, pp. 817–822.
[23] H.K. Khalil, Nonlinear Systems, Prentice–Hall, New Jersey, 1996.
[24] C.-T. Chen, Linear System Theory and Design, Oxford University Press, 1999.
[25] V. Zakian, Control Systems Design, Springer, 2005.